[19]Duco Household Cement, E. I. du Pont de Nemours and Co., Inc., Wilmington, Delaware.
[20]Castolite Co., Woodstock, Illinois.
[21]0–50-atm gauge, calibrated in 0.05-atm steps. Heise-Bourdon Tube Company, Newtown, Connecticut.
[22]K. N. Zinovieva, Zh. Eksperim. i Teor. Fiz. 44, 1837 (1963) [English transl.: Soviet Phys. – JETP 17, 1235 (1963)].
[23]R. L. Mills, E. R. Grilly, and S. G. Sydoriak, Ann. Phys. 12, 41 (1961).
[24]I. Prigogine and R. Defay, Chemical Thermodynamics (Longman's Green and Co., Inc., New York, 1954) p. 71.
[25]R. C. Richardson, E. Hunt, and H. Meyer, Phys. Rev. 138, A1326 (1965).
[26]M. F. Panczyk, R. A. Scribner, G. C. Straty, and E. D. Adams, Phys. Rev. Letters 19, 1102 (1967).
[27]L. D. Landau and E. M. Lifshitz, Statistical Physics (Pergamon Press, Ltd., New York, 1960) p. 310.
[28]See Ref. 24, p. 281.
[29]E. H. Graf, D. M. Lee, and J. D. Reppy, Phys. Rev. Letters 19, 417 (1967).
[30]F. P. Lipschultz, P. M. Tedrow, and D. M. Lee, in Proceedings of the Ninth International Conference on Low Temperature Physics, Columbus, 1964, edited by J. G. Daunt *et al.* (Plenum Press, Inc., New York, 1965), p. 254.
[31]N. G. Berezniak, I. V. Bogoyavlensky, and B. N. Eselson, Zh. Eksperim. i Teor. Fiz. 45, 486 (1963), [English transl.: Soviet Phys. – JETP 18, 335 (1964)].

PHYSICAL REVIEW VOLUME 181, NUMBER 1 5 MAY 1969

Heat of Mixing and Ground-State Energy of Liquid He^3-He^4 Mixtures*

P. Seligmann, D. O. Edwards, R. E. Sarwinski, and J. T. Tough
Department of Physics, Ohio State University, Columbus, Ohio 43210
(Received 24 January 1969)

The heat evolved when He^3 is added to liquid He^3-He^4 mixtures at the saturated vapor pressure has been measured for temperatures in the region of 0.05°K. The starting concentrations varied between zero and six atomic percent of He^3. Since the variation of the energy with temperature (the specific heat) is known, the experiments give the ground-state energy and the He^3 and He^4 chemical potentials at 0°K as a function of concentration. The measurements were made in a calorimeter connected by a wire of high thermal resistance to a dilution refrigerator operating at ~0.02°K. The He^3 was added through a long tube containing thermal anchors connected to the refrigerator.

The results give the difference in binding energy for one He^3 atom in He^4 relative to pure He^3 as $(E_3 - L_3{}^0)/k_B = (0.312 \pm 0.007)$ deg K, in excellent agreement with the theoretical value of Massey and Woo. The concentration dependence of the energy and chemical potentials agrees with predictions using the Bardeen, Baym, and Pines empirical interaction. The osmotic pressure in a saturated solution at 0°K is found to be (17.8 ± 0.9) mm Hg.

INTRODUCTION

In the experiment described here, we have measured as directly as possible the ground-state or 0°K energy of He^3-He^4 solutions as a function of X, the atomic concentration of He^3. The measurements have been carried out at zero pressure up to the limit of solubility of He^3 in He^4 which, according to the results of Ifft *et al.*,[1] is $X_0 = 6.4\%$. The present experiment was primarily undertaken to determine the binding energy of one He^3 atom in liquid He^4 (E_3 in our notation) to compare with recent theoretical estimates.[2–5] In addition, the variation of the ground-state energy with concentration and the derived chemical potentials at 0°K, $\mu_{30}(X)$ and $\mu_{40}(X)$, provide an excellent test of the empirical quasiparticle effective interaction constructed by Bardeen, Baym, and Pines (BBP).[3,6]

Theory of the Experiment

The energy of a mole of mixture at 0°K, $H_0(X)$, is conveniently described by the excess energy (or enthalpy, since $p = 0$), $H_0{}^E$, defined so that

$$H_0(X) = XH_0(X=1) + (1-X)H_0(X=0) + H_0{}^E(X)$$
$$= -XN_A L_3{}^0 - (1-X)N_A L_4{}^0 + H_0{}^E(X). \quad (1)$$

Here L_3^0 and L_4^0 are the latent heats per atom of pure He^3 and pure He^4 at 0°K, and N_A is Avogadro's number. Empirically[7-9] the specific heat of a dilute solution of He^3 in He^4 below about 0.4°K is very close to that of a Fermi gas with the same number density $n_3(X)$ and with an effective mass m^*. The mass $m^*(X)$ varies slightly with concentration,[8,9] but is of the order of 2.4 times the real mass of He^3. Therefore

$$H(X,T) = H_0(X) + \int_0^T XC_F(T', T_F)\,dT'$$
$$= H_0(X) + X[U_F(T, T_F) - U_F(0, T_F)]$$
$$= H_0(X) + X\Delta U_F(T, T_F), \quad (2)$$

where the Fermi temperature T_F is calculated from the empirically determined[1] He^3 number density $n_3(X)$ and the equation

$$k_B T_F = (\hbar^2/2m^*)(3\pi^2 n_3)^{2/3}. \quad (3)$$

Tables of the specific heat at constant volume C_F, internal energy U_F, and other thermodynamic functions of the ideal Fermi gas have been published by Stoner.[10]

The experiment we have performed consists of adding known quantities of liquid He^3 to a mixture and measuring the initial and final temperatures and the heat lost to the surroundings Q. Suppose the average temperature of the incoming He^3 is T_3, the initial and final temperatures and concentrations are T_i, X_i and T_f, X_f, and the number of moles of He^4 is N_4; then conservation of energy gives

$$\delta[H_0^E/(1-X)] + \delta[X\Delta U_F/(1-X)] + Q/N_4$$
$$= h_3(T_3)\delta[X/(1-X)]. \quad (4)$$

Here

$$\delta[H_0^E/(1-X)] = H_0^E(X_f)/(1-X_f) - H_0^E(X_i)/(1-X_i),$$

$$\delta[X\Delta U_F/(1-X)] = X_f \Delta U_F(T_f, T_{Ff})/(1-X_f)$$
$$- X_i \Delta U_F(T_i, T_{Fi})/(1-X_i),$$

$$\delta[X/(1-X)] = X_f/(1-X_f) - X_i/(1-X_i),$$

and $h_3(T_3) = \int_0^{T_3} C_3(T)dT$, the temperature-dependent part of the enthalpy of pure He^3.

By starting with pure $He^4(X_i = 0)$ and adding successive amounts of He^3 so that the final concentration for the jth mixing $X_{f,j}$ was the initial concentration for the next $X_{i,j+1}$, we were able to obtain $H_0^E(X)$ from

$$H_0^E/(1-X) = \sum \delta[H_0^E/(1-X)]$$
$$= \sum_{j=1}^{n} [H_0^E(X_{f,j})/(1-X_{f,j}) - H_0^E(X_{i,j})/(1-X_{i,j})], \quad (5)$$

where $X_{i,1} = 0$ and $X_{f,n} = X$.

In using Eq. (4) the Fermi temperatures were obtained from Eq. (3) with the values of $m^*(X)$ calculated by Radebaugh.[11] Although these were derived using the theory of Bardeen, Baym, and Pines, they can be considered as a semi-empirical fit to the measured specific heats. The values of $h_3(T)$ used in Eq. (4) were also taken from Radebaugh who derived them from empirical specific heat data.

EXPERIMENTAL

Apparatus and Procedure

The mixing was performed in an epoxy calorimeter cell containing finely powdered cerium magnesium nitrate for magnetic thermometry. The heat capacity of the calorimeter was always negligible compared to that of the He^3 in solution. After the calorimeter was partially filled with about 6 cm^3 of pure liquid He^4, the He^3 was added through many meters of spiralled 0.0127-cm-diam filling tube containing a number of sintered-copper thermal anchors. The coldest anchor, at about 0.06°K, was connected to a heat exchanger of a dilution refrigerator and its temperature was measured by a Speer 220-Ω carbon thermometer. An independent check on the temperature of the incoming He^3, T_3, was made in separate, control experiments when He^3 was added to a saturated mixture (see below). A brush of 10,000 copper wires in contact with the helium in the cell was connected through a large thermal resistance, a 24-cm length of 0.0254-cm-diam copper wire and two mechanical contacts, to the mixing chamber of the dilution refrigerator which was at ~0.02°K. The thermal time constant of the system formed by the helium heat capacity and the thermal resistance of the wire was many hours and therefore greater than the time required to perform a mixing (see Fig. 1).

The initial temperatures for the solution varied between 0.05 and 0.062°K. For solutions with low initial concentrations, the temperature rose as high as 0.13°K during the mixing. For solutions of high concentration, the temperature change was much smaller, since $\delta[H_0^E/(1-X)]$ decreases and the heat capacity increases with concentration. For these higher concentration experiments Q, the heat loss from the cell to the refrigerator, was small, and the heat introduced by the pure He^3 had

a large effect on the result for $\delta[H_0^E/(1-X)]$.

The heat loss in each mixing Q was determined from the graph of the cell temperature versus time, Fig. 1, and the measured properties of the thermal link between the cell and the refrigerator. The link was calibrated using an electric heater in the cell. It was found that the rate of heat loss $\dot{Q}$ was given within the scatter of the measurements by the empirical equation $\dot{Q} = (389T^{7/3} - 0.24)$ ergs/sec, and that $\dot{Q}$ depended only on the temperature of the cell T and was independent of the concentration of the liquid helium in it. In addition, a preliminary experiment was performed in which the long copper wire was replaced by a good thermal contact, so that the other thermal resistances inside the cell and at the mixing chamber of the refrigerator could be investigated. The variation of the thermal resistance inside the cell with concentration was proved to be negligible compared to the resistance of the link used in the mixing experiment. The effect of temperature changes in the dilution refrigerator was also proved to be negligible. The main sources of error in $\dot{Q}$ and in the integrated heat loss Q were changes in the background heating to the cell amounting to less than ± 0.1 ergs/sec.

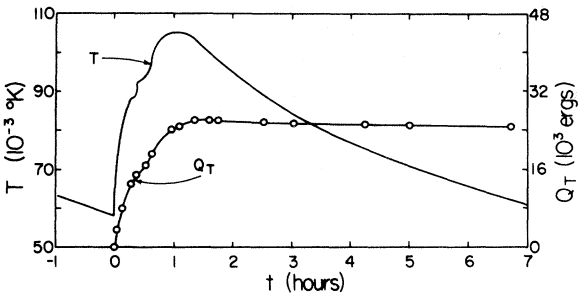

FIG. 1. Temperature T and the quantity of heat Q_T defined by Eq. (6) as a function of time during mixing-measurement number three.

To check the consistency of the data, observations of the temperature were taken long after all of the He^3 had arrived in the cell so that we had a series of values of $Q(t)$ and $T_f(t)$. Since, after all the He^3 has arrived, X is constant and equal to X_f, the quantity

$$Q_T = Q(t) + X_f[N_4/(1-X_f)] \int_{T_i}^{T_f(t)} C_F dT \qquad (6)$$

should then be independent of time. When plotted against time, the empirical values of Q_T usually showed a small systematic decrease with t, as seen in Fig. 1, but within the ± 0.1 ergs/sec uncertainty in the heat loss $\dot{Q}$. We have no explanation of why the effect was systematic, but it was taken into account in estimating the accuracy of the results.

The time for the added He^3 to arrive at the cell after being admitted to the room-temperature end of the filling line varied from a few minutes to two hours. It depended, among other things, on the amount of He^3 added, which controlled the hydrostatic pressure available to push the liquid through the sintered-copper thermal anchors and the long spirals of tubing. It was assumed that all of the He^3 had entered the cell after Q_T had become nearly constant. In the preliminary experiment in which the cell was attached to the refrigerator with a good thermal contact, 25×10^{-6} moles of pure He^3 were added to pure He^4. This quantity of He^3 was 1% to 3% of the amount added during a typical mixing experiment. After $4\frac{1}{2}$ h the arrival of the He^3 in the cell was detected by the change in the thermal resistance between the cell and the refrigerator.

It was concluded from this experiment that during a mixing measurement only a negligible amount of He^3 could be trapped in the fill line or otherwise fail to reach the cell.

Control Experiments and Errors

A series of control experiments were made to check the accuracy of our temperature and concentration measurements and the assumption that the heat capacity of the helium was the same as that of a Fermi gas. Instead of adding He^3, a measured amount of electrical heating was applied to the cell, enough to raise the temperature from about 0.05°K to about 0.1°K, and the initial and final temperatures T_i and T_f and the heat loss Q were measured. The results of these measurements, made at three concentrations, have been used to calculate the values of the effective mass $m^*(X)$ shown as closed circles in Fig. 2. As the figure shows, the measurements are in excellent agreement with Radebaugh's curve[11] which we have used to interpret the mixing data. On the other hand, Radebaugh's curve was calculated from the effective interaction of Ebner[12] which is now known to be too strong.[6] The full curve, which has been calculated from the original BBP potential[3] reduced by a factor of $(\frac{3}{4})^{1/2}$ to agree with recent more accurate equations for the transport properties,[6] has been fitted to all the specific heat measurements presently available and indicates that the effective mass for $X=0$, $m^*(0)$, is equal to $2.36m_3$. This is not significantly different from the earlier fit by BBP which gave $m^*(0) = 2.34m_3$. Two of the control measurements of m^* were performed immediately after the mixing experiments. The excellent agreement between the present values of m^* and those determined in previous specific heat measurements indicates that the uncertainties in concentration are small.

The most important uncertainty in the present experiment is probably associated with T_3, the

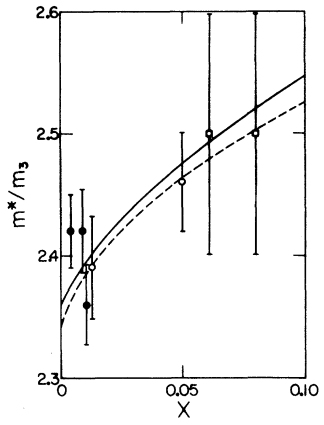

FIG. 2. The He^3 effective mass ratio $m^*(X)/m_3$ in solution as a function of concentration. The open circles are from Anderson *et al.* (Ref. 9), the squares have been estimated from the data of Edwards *et al.* (Ref. 7), and the closed circles are from the control measurements in the present experiment. The dashed curve was calculated by Radebaugh (Ref. 11) using Ebner's potential and $m^*(0) = 2.34 m_3$. The full curve was calculated using $(\frac{3}{4})^{1/2}$ times the BBP potential and $m^*(0) = 2.36\ m_3$.

average temperature of the incoming He^3. Normally this was monitored by the carbon resistor, but in two control experiments T_3 was obtained in a more reliable way: He^3 was added to a saturated two-phase mixture, so that at constant temperature it would not dissolve but would go into the almost pure[1] upper phase. In this case, if the rise in temperature $T_f - T_i$ is small, and the number of moles of He^3 is increased from N_3 to $N_3 + \delta N_3$,

$$C(\bar{T})(T_f - T_i) + Q = \delta N_3[h_3(T_3) - h_3(T_f)], \quad (7)$$

where $\bar{T} = \frac{1}{2}(T_i + T_f)$ and the heat capacity $C(T)$ is given by

$$C(T) = N_3{}^l C_F + N_3{}^u C_3 + N_3{}^l \left(\frac{S_F - S_3}{1 - X^l} - C_F \frac{\partial \ln T_F}{\partial \ln X^l} \right) \frac{d \ln X^l}{d \ln T}. \quad (8)$$

In Eqs. (7) and (8) we have used the same notation as in the Introduction, and also the assumption that the upper phase is pure He^3. The number of moles of He^3 in the lower phase is $N_3{}^l(T) = X^l N_4/(1 - X^l)$; the number in the upper phase initially is $N_3{}^u(T) = N_3 - N_3{}^l$. The last term in Eq. (8) is small at $T \sim 0.05$°K and is easy to evaluate, since in this temperature range[1] X^l is given by

$$X^l = 0.064[1 + (10.8\ \text{deg}^{-2}) T^2]. \quad (9)$$

Two experiments of this type were performed: In the first, the incoming He^3 took 2000 sec to reach the cell, the carbon thermometer gave $T_3 = 0.074$°K while the value derived from Q, T_i, and T_f using Eqs. (7) to (9) was 0.073°K. In the second, the He^3 arrived in 200 sec, the carbon thermometer gave 0.076°K, while T_3 from the "mixing" experiment was 0.086°K. The uncertainty in T_3 is most important for the high-concentration mixing experiments where the heat of mixing is small. For these the arrival times were all of the order of 200 sec, so that it was decided to scale up the carbon thermometer readings for all experiments as indicated by the second control experiment. The discrepancy between the carbon thermometer value of T_3 and that given by the second control experiment was used in estimating the accuracy of the data.

Two other possible sources of error should be mentioned: Calculation shows that there may have been a small amount of frictional heating as the liquid He^3 passed through the final section of the filling tube. The values of T_3 obtained from the control experiments take this effect into account. Secondly, the action of the He^4 superfluid film tends to dilute the incoming He^3. The magnitude of this effect should depend on the time taken for the He^3 to travel down the filling tube. The results for experiments with $X_f = 0.451\%$, which took 2340 sec, and with $X_f = 0.556\%$, which took 660 sec, are consistent to 1% of $\delta[H_0{}^E/(1 - X)]$, showing that the effect is probably negligible.

RESULTS AND DISCUSSION

The Energy

The results of the measurements of X_i, X_f, and $\delta[H_0{}^E/(1 - X)]$ are given in Table I. The experimental errors quoted are from all sources including the uncertainties in the values of T_3, m^*, and the effect of the He^4 film in the filling tube. For point number 6, an excess of He^3 was added so that two phases were formed. The value of X_f quoted in parentheses for point 6 is the concentration in the lower phase at T_f, obtained from the data of Ifft *et al.*[1] using Eq. (9). To calculate $\delta[H_0{}^E/(1 - X)]$ for this point, Eq. (4) was modified to take into account the fact that not all of the added He^3 dissolved in the lower phase.

Values of the excess energy $H_0{}^E$, derived from the data using Eq. (5), are given in Table II. The gaps in the series of concentrations in points 1 to 6 in Table I, between $X = 0$ and $X = 0.0175\%$ and between $X = 0.451\%$ and $X = 0.753\%$, were filled by interpolation with the aid of points 7 and 8. The interpolation was made on a graph of $H_0{}^E - \frac{3}{5} X R T_F$ which, as we shall see below, is very nearly linear in X. The interpolations introduce negligible additional error in the data. In calculating the

TABLE I. Values of X_i, X_f, and $\delta[H_0^E/(1-X)]/R$.

Measurement number	1	2	3	4	5	6	7	8
10^2X_i	0.0175	0.753	1.075	2.006	3.996	5.805	0.000	0.556
10^2X_f	0.451	1.075	2.006	3.996	5.805	(6.60)[a]	0.556	0.920
$\delta[H_0^E/(1-X)]/R$ (mdegK)	$(1.17_0 \pm 0.01_5)$	$(0.68_1 \pm 0.02_9)$	(1.66 ± 0.06)	$(2.3_7 \pm 0.1_3)$	$(1.0_5 \pm 0.0_9)$	$(0.20_5 \pm 0.05)$	$(1.51_0 \pm 0.01_5)$	$(0.80_9 \pm 0.00_5)$

[a] X^l

TABLE II. The ground-state excess energy H_0^E as a function of concentration X.

10^2X	0.451	0.556	0.920	1.075	2.01	4.00	5.81	6.60
H_0^E/R (mdegK)	$(-1.21_4 \pm 0.01_5)$	$(-1.50 \pm 0.01_5)$	(−2.30 ± 0.02)	(−2.60 ± 0.04)	(−4.20 ± 0.10)	(−6.4 ± 0.2)	(−7.3 ± 0.3)	(−7.4 ± 0.4)

other errors in H_0^E, we have assumed most of them to be systematic and cumulative.

An important result in the Bardeen, Baym, and Pines[3] (BBP) theory of He^3 in solution is that the chemical potential at 0°K is modified from the Landau-Pomeranchuk ideal-gas form according to the equation:

$$\mu_{30} = -E_3 + k_B T_{F0} + n_3 V_0 - \frac{6n_3}{(2k_F)^3}\int_0^{2k_F}\left(1-\frac{k'}{2k_F}\right)V_{k'}k'^2dk'. \quad (10)$$

In Eq. (10) the Fermi temperature T_{F0} is

$$k_B T_{F0} = \hbar^2 k_F^2/2m_0^* = (\hbar^2/2m_0^*)(3\pi^2 n_3)^{2/3},$$

where m_0^* is the effective mass at zero He^3 concentration, $m_0^* = m^*(X=0) = 2.34m_3$. The binding energy per atom E_3 is defined so that the energy-momentum relation for *one* He^3 quasiparticle in solution is

$$\epsilon = -E_3 + \hbar^2k^2/2m_0^*. \quad (11)$$

The quantity V_k is the Fourier transform of the effective interaction between He^3 quasiparticles. It is related to the interaction in ordinary space $V(\vec{r})$ by

$$V_k = \int V(r)e^{i\vec{k}\cdot\vec{r}}dr, \quad (12)$$

so that $V_0 = \int V(r)d\vec{r}$.

By using the Gibbs-Duhem relation $n_3 d\mu_{30} = -n_4 d\mu_{40}$ and the fact that $\mu_{40}(X=0) = -L_4^0$, we can obtain the He^4 chemical potential

$$(\mu_{40} + L_4^0)/X = -\tfrac{2}{5}k_B T_{F0}[1 + \tfrac{5}{8}X(1-\tfrac{3}{5}\alpha)] - \tfrac{1}{2}n_3 V_0 + [3n_3/(2k_F)^4] \times \int_0^{2k_F} F[1-(k'^2/4k_F^2)]V_{k'}k'^3dk'. \quad (13)$$

This result was first given by Ebner.[13]

In deriving Eq. (13) we have used the empirical result that $n_3 = Xn_4^0/(1+\alpha X)$ where n_4^0 is the number density of pure He^4. The constant α has been determined by Ifft *et al.*[1] to be 0.284 ± 0.005. We have also discarded small terms of order Xn_3V_0. To the same degree of accuracy, Eqs. (10) and (13) can be combined to give the excess enthalpy at 0°K, H_0^E,

$$\frac{H_0^E}{N_A X} = -(E_3 - L_3^0) + \tfrac{3}{5}k_B T_{F0}[1 + \tfrac{1}{4}(1+\alpha)X] + \tfrac{1}{2}n_3 V_0 - [3n_3/(2k_F)^3] \times \int_0^{2k_F}\left(2 - \frac{3k'}{2k_F} + \frac{k'^3}{(2k_F)^3}\right)V_{k'}k'^2dk'. \quad (14)$$

According to Eq. (14) a graph of $H_0^E/RX - \frac{3}{5}T_{F0}[1+\frac{1}{4}(1+\alpha)X]$ versus X or n_3 should have $-(E_3 - L_3^0)/k_B$ as intercept as $X \to 0$. This is shown in Fig. 3 which we have used to estimate that

$$(E_3 - L_3^0)/k_B = (0.312 \pm 0.007) \text{ deg K}. \quad (15)$$

Using the best value of $L_3^0/k_B = (2.473 \pm 0.009)$ deg K,[14] this gives $E_3/k_B = (2.785 \pm 0.011)$ deg K. This is in impressive agreement with the latest perturbation calculation by Massey and Woo[5] which gives $E_3/k_B = 2.79$ deg K. Figure 3 also shows the theoretical values of the last two terms in Eq. (14), calculated with the latest potential function V_k, that derived by Baym and Ebner[6] from thermal conductivity and spin-diffusion measurements. The agreement is very satisfactory and well within experimental error.

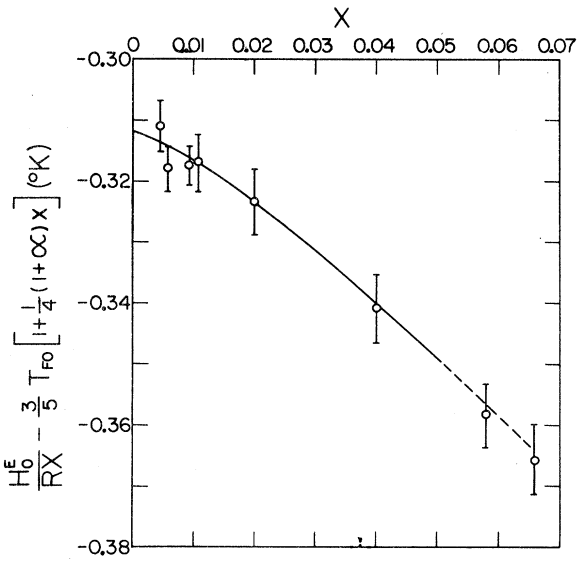

FIG. 3. The excess ground-state energy from the present measurements (circles) plotted as

$$H_0^E/RX - \tfrac{3}{5} T_{F0}[1+\tfrac{1}{4}(1+\alpha)X]$$

versus X. The variation of this quantity is due to the effect of the quasiparticle interaction. The curve is theoretical, calculated from the empirical potential of Baym and Ebner (Ref. 6) and the present experimental value of $\mu_{30}+L_3{}^0$ at $X=0$.

The He^3 Chemical Potential and Phase Separation at 0°K

The chemical potentials at 0°K are related to the excess enthalpy by the thermodynamic equations

$$N_A[\mu_{30}(X)+L_3{}^0] = (1-X)^2 \frac{d[H_0^E/(1-X)]}{dX}, \qquad (16)$$

$$N_A[\mu_{40}(X)+L_4{}^0] = \frac{H_0^E}{1-X} - X(1-X)\frac{d[H_0^E/(1-X)]}{dX}. \qquad (17)$$

To calculate μ_{30} and μ_{40} from the data, we replaced the derivative $d[H_0^E/(1-X)]/dX$ by $\delta[H_0^E/(1-X)]/\delta X$ evaluated at $X=\bar{X}=(X_f+X_i)/2$. It is easy to show that this approximation involves only a negligible error.

The He^3 chemical potential at 0°K, μ_{30}, is shown in Fig. 4 and Table III. In a saturated solution of concentration X_0, which is in equilibrium with pure He^3 at 0°K,

$$\mu_{30}(X_0) = \mu_{30}^{\text{pure}} = -L_3{}^0$$

so that $\mu_{30}(X_0)+L_3{}^0=0$. According to the measurements of Ifft *et al.*,[1] $X_0=(6.40\pm0.07)\%$. The present data are in only moderate agreement with this result since the extrapolated value of $(\mu_{30}+L_3{}^0)/k_B$ at 6.4% is (-18 ± 8) mdeg K instead of zero. The discrepancy is outside the estimated experimental error, and it is not understood. We believe that it is due to uncertainties in the value of T_3, the temperature of the incoming He^3, which is

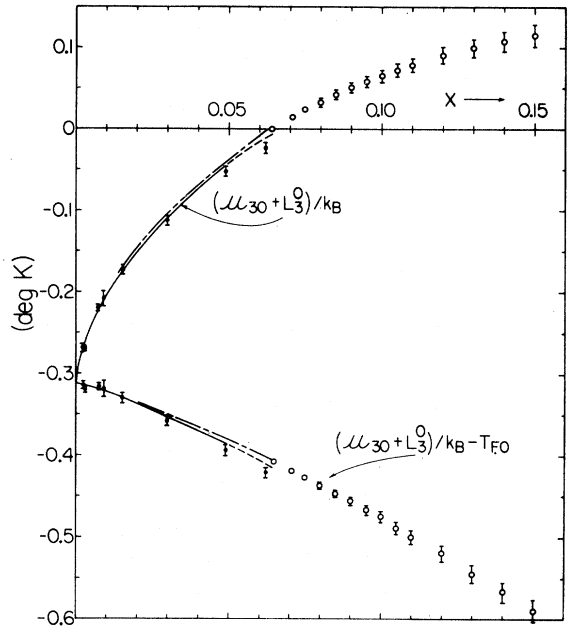

FIG. 4. The excess He^3 chemical potential at 0°K, $(\mu_{30}+L_3{}^0)/k_B$ and the contribution from the interaction, $(\mu_{30}+L_3{}^0)/k_B - T_{F0}$, as a function of concentration. The open circles were calculated from the data of *Ifft et al.* (Ref. 1); the solid circles are the present data. The theoretical curves are calculated from the empirical potential of Baym and Ebner (full curve) and $(\frac{3}{4})^{1/2}$ times the potential of Bardeen, Baym, and Pines (broken curve).

TABLE III. The ground-state chemical potentials as a function of He^3 concentration X.

10^2X	0.234	0.278	0.738	0.914	1.54	3.00	4.91	6.20
$(\mu_{30}+L_3{}^0)/R$ (mdegK)	(−269 ± 4)	(−269 ± 3)	(−219 ± 3)	(−208 ± 9)	(−173 ± 7)	(−112 ± 7)	(−52 ± 5)	(−23 ± 6)
$(\mu_{40}+L_4{}^0)/R$ (mdegK)	(0.00 ± 0.02)	(−0.00 ± 0.02)	(−0.29 ± 0.02)	(−0.37 ± 0.05)	(−0.75 ± 0.08)	(−2.0 ± 0.2)	(−4.5 ± 0.3)	(−6.3 ± 0.5)

very important for the measurements at higher concentrations, near to saturation.

We have also calculated μ_3 at 0°K from the measurements of Ifft *et al.*[1] In their second paper they give a table of $\mu_3(X, T)+L_3^0$ along the phase-separation line. Their values of μ_3 may be reduced to 0°K by using the same assumption as we have used throughout this work; that the specific heat is that of an ideal gas with concentration-dependent effective mass. It then follows that the entropy $S=XS_F$. From

$$-N_A\frac{\partial\mu_3}{\partial T}=XS_F+(1-X)\frac{\partial(XS_F)}{\partial X},$$

we can derive

$$N_A[\mu_3(X,T)-\mu_{30}(X)]=\Delta G_F+[(1-X)(d\ln T_F/d\ln X)-\tfrac{2}{3}]\,\Delta U_F. \quad (18)$$

This equation can also be used to derive μ_3 at finite temperatures from the present values of μ_{30}. The second term on the right in Eq. (18) is a small correction to the first, since $(d\ln T_F)/(d\ln X)\approx\frac{2}{3}$. The results of applying Eq. (18) to the data of Ifft *et al.*[1] are shown as open circles in Fig. 4. The error limits are due to uncertainties in the data and in the term $(d\ln T_F)/(d\ln X)$.

It is interesting to observe that $\mu_{30}+L_3^0$ in Fig. 4 continues to increase over the whole range of concentration. This means that solutions between 6.4 and 16% are, in principle, metastable unless some nucleus of concentration much greater than 16% can be formed in the liquid. We note also that the effect discussed by Andreev,[15] namely the existence of a film of He^3 at the liquid-vapor surface, probably means that nucleation can proceed from any free surface of the liquid. On the other hand, it is well known that the opposite effect occurs at any solid-liquid boundary: the liquid is enriched in He^4 by the action of the van der Waals forces, so that the walls of the vessel, dust particles, etc., are unlikely to be effective in nucleating the concentrated phase. We therefore should expect to see supercooling of the single-phase liquid when the filling line to the vessel is completely filled with liquid up to a temperature outside the two-phase region. Supercooling under these conditions has recently been observed and will be described in a future publication.

Figure 4 also shows two theoretical curves calculated using the BBP equation, Eq. (10). These are the full curve, based on the latest V_k derived by Baym and Ebner,[6] and the dashed curve based on the original BBP V_k multiplied by $(\frac{3}{4})^{1/2}$ to bring it into agreement with the variational calculation for the spin diffusion coefficient.

Both theoretical curves have been fitted to the experimental value of $\mu_{30}(X=0)+L_3^0$, namely -0.312 deg K. The Baym and Ebner formula cannot be extended reliably beyond the concentration range in which the transport data were fitted, 0 to 5%. The modified BBP form can be extrapolated with slightly more confidence, but again it was fitted to spin diffusion data at 1.3% and 5%. Remembering that the present data are probably somewhat in error near 6.4% as discussed above, the agreement between theory and experiment is very good.

The Osmotic Pressure at 0°K

The He^4 chemical potential is shown in Table III and in terms of the osmotic pressure at 0°K, π_0, in Fig. 5. We have calculated π_0 from the relation[16]

$$-\pi_0 v_4^0=N_A[\mu_{40}(X)+L_4^0], \quad (19)$$

where v_4^0 is the molar volume of pure He^4 at $p=0$. The open circles were obtained from the present data using Eq. (17). The closed circle represents

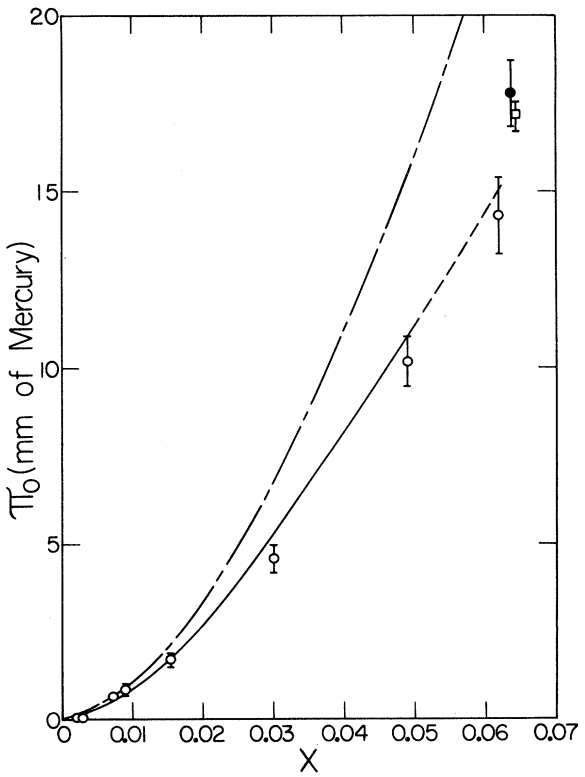

FIG. 5. The osmotic pressure at 0°K as a function of concentration. Open circles: present data; closed circles: the osmotic pressure at saturation from the present data; square: London *et al.* (Ref. 17). The full curve has been calculated with Eqs. (13) and (19) from the empirical potential of Baym and Ebner; the broken curve has been calculated assuming $V_k=0$.

a value of π_0 for the saturated solution of concentration X_0. It has been calculated from Eq. (17) putting the term in $d[H_0^E/(1-X)]/dX$ equal to zero, so that $(\mu_{30}+L_3^0)$ is zero as required by Eq. (16); that is,

$$-\pi_0(X_0)v_4^0 = N_A[\mu_{40}(X_0)+L_4^0] = H_0^E(X_0)/(1-X_0). \quad (20)$$

We have taken X_0 to be 6.4% as measured by Ifft *et al.*,[1] but in fact the value of $\mu_{40}(X_0)$ given by Eq. (20) is not very sensitive either to X_0 or to the measurements of $\delta[H_0^E/(1-X)]$ near to X_0 which, as we have seen, are probably in error. We have also plotted $\pi_0(X_0)$ as measured recently by London, Phillips, and Thomas[17] (square) which is in excellent agreement with the result from Eq. (20). Both the values for $\pi_0(X_0)$ have been plotted at $X = 6.4\%$ (London *et al.* did not measure X_0) and they are consequently somewhat higher than an extrapolation of the data from Eq. (17), which is only consistent with a higher value of X_0. As remarked before, we believe this to be caused by a possible systematic error in T_3 for the experiments at high concentrations.

The value of $\pi_0(X_0)$ at 0°K has some relevance to the operation of dilution refrigerators. In a refrigerator the concentration in the still X_S is determined by the equality of the He^4 chemical potentials in the still and the mixing chamber:

$$\mu_4(T_S, X_S, p) = \mu_4(T_m, X_m, p) .$$

For a mixing-chamber temperature T_m below ~0.04°K,

$$\mu_4(T_m, X_m) \approx \mu_4(0, X_0) ,$$

while as Wilson *et al.*[16] showed, for T_S between 0.3°K and 0.85°K,

$$\mu_4(T_S, X_S) = -L_4^0 - X_S R T_S .$$

Taking our value of $\pi_0(X_0)$, (17.8 ± 0.9) mm Hg, this gives $X_S T_S = (0.79 \pm 0.04)\%\,°K$.

The full curve in Fig. 5 is the theoretical result from Eq. (13), using the V_k constructed by Baym and Ebner. The agreement is certainly within experimental error, and furthermore, it does not depend on any adjustable constants. To give some idea of the influence of the effective interaction on π_0, we have drawn the broken curve which represents Eq. (13) with the terms in V_0 and V_k put equal to zero. The broken curve can therefore be regarded as the osmotic pressure for an "ideal" non-interacting solution.

CONCLUSION

The agreement between the BBP theory using the most recent V_k determined from transport coefficients and the experimental energy and chemical potentials is within about 5%. This is approximately the experimental uncertainty in the contribution from V_k to the energy.

The single-particle binding energy E_3 is also in excellent agreement with the value from perturbation theory. At the present time the accuracy with which E_3 can be determined is limited by the uncertainty in the latent heat of pure He^3.

ACKNOWLEDGMENTS

We are grateful to W. Baker, R. Kindler, and L. Wilkes for their technical assistance.

---

*Work supported by the National Science Foundation.

[1]E. M. Ifft, D. O. Edwards, R. E. Sarwinski, and M. M. Skertic, Phys. Rev. Letters 19, 831 (1967); D. O. Edwards, E. M. Ifft, and R. E. Sarwinski, Phys. Rev. 177, 380 (1969).

[2]G. Baym, Phys. Rev. Letters 17, 952 (1966).

[3]J. Bardeen, G. Baym, and D. Pines, Phys. Rev. 156, 207 (1967).

[4]W. E. Massey and C. W. Woo, Phys. Rev. Letters 19, 301 (1967).

[5]W. E. Massey and C. W. Woo, to be published.

[6]G. Baym and C. Ebner, Phys. Rev. 170, 346 (1968).

[7]D. O. Edwards, D. F. Brewer, P. Seligmann, M. Skertic, and M. Yaqub, Phys. Rev. Letters 15, 773 (1965).

[8]A. C. Anderson, W. R. Roach, R. E. Sarwinski, and J. C. Wheatley, Phys. Rev. Letters 16, 263 (1966).

[9]A. C. Anderson, D. O. Edwards, W. R. Roach, R. E. Sarwinski, and J. C. Wheatley, Phys. Rev. Letters 17, 367 (1966).

[10]E. C. Stoner, Phil. Mag. 28, 257 (1939).

[11]R. Radebaugh, National Bureau Standards Report No. 362 (U.S. Government Printing Office, Washington, 1967).

[12]C. Ebner, Phys. Rev. 156, 222 (1967).

[13]C. Ebner, Ph.D. Dissertation, University of Illinois, 1967 (unpublished).

[14]T. R. Roberts, R. H. Sherman, and S. G. Sydoriak, J. Res. Natl. Bur. Std. (U.S.) 68A, 567 (1964).

[15]A. F. Andreev, Zh. Eksperim. i Teor. Fiz. (USSR) 50, 1415 (1966); [English Transl.: Soviet Physics – JETP 23, 939 (1966)].

[16]M. F. Wilson, D. O. Edwards, and J. T. Tough, Phys. Rev. Letters 19, 1368 (1968).
[17]H. London, D. Phillips, and G. P. Thomas, in "Proceedings of the Eleventh International Conference on Low Temperature Physics, St. Andrews, Scotland, 1968" (to be published by the organising committee of the Conference, St. Andrews, Scotland, 1968).

PHYSICAL REVIEW VOLUME 181, NUMBER 1 5 MAY 1969

Temperature Decay and Recombination in Helium Afterglow Plasmas

Gunhard K. Born and Rudolf G. Buser
Institute for Exploratory Research, U. S. Army Electronics Command, Fort Monmouth, New Jersey 07703
(Received 24 April 1967; revised manuscript received 6 January 1969)

The effect of the temperature of the neutral gas on the decay of electron temperature and density in helium afterglow plasmas ($p = 0.3$–0.7 Torr, $N_e \approx 10^{13}$ cm^{-3}, $T_e \approx 2000°$K) is investigated. Density and temperature of the electrons and the concentration of metastable atoms are measured with optical and microwave methods; the gas temperature is determined from standing acoustic waves excited by the discharge. In the investigated range no difference is found during the afterglow between the temperatures of the electrons and of the gas which is heated in the discharge. The slow electron-temperature decay follows the decay of the elevated gas temperature controlled by heat conduction, and is not affected by electron-heating processes due to metastable atoms and recombination. With collisional-radiative recombination as the major plasma loss mechanism, the plasma decay can be approximately predicted from the initial density and temperature.

I. INTRODUCTION

In dense helium afterglow plasmas ($\approx 10^{13} e/\text{cm}^3$), it has been possible to study volume recombination relatively undisturbed by diffusion effects. The plasma decay in various experiments[1–8] has been successfully explained by an electron-ion recombination mechanism in which electron-electron-ion collisions and collision-induced transitions in excited atoms play an important role.[3,9–11] This process, called "collisional-radiative recombination,"[10] depends strongly on the electron temperature. The experimental recombination rates, related to the corresponding measured electron temperatures, have substantially confirmed the theoretical results.[3,10,11] To obtain a complete description of the plasma disintegration, attempts have also been made to predict the time-varying electron temperature from the initial conditions of the early afterglow. The temperature decay was usually found slow compared with the theoretical cooling rates so that different afterglow electron-heating mechanisms have been proposed. Helium atoms in metastable states approximately 20 eV above the ground level constitute a major reservoir of energy which may be released during the afterglow by collisional relaxation processes.[2,12] Heating occurs also as a consequence of the collisional recombination reaction in which the free electrons may carry the excess recombination energy away.[13] Most extensive calculations of the quasiequilibrium electron temperatures resulting from the simultaneous heating and cooling processes in hydrogen plasmas have been conducted by Bates and Kingston for a wide range of experimental parameters, including different temperatures of the neutral gas.[14] They also gave some results for helium plasmas with the gas at room temperature.

For a complete analysis of afterglows the correct gas temperature has to be used. The usual assumption that the gas remains at room temperature seems only justified in experiments where the applied discharge energy is too low for a significant heating, or where (in magnetically confined plasmas) the pressure is low enough for a rapid dissipation of the acquired energy. These conditions are usually not fulfilled if dense plasmas are to be generated by gas discharges in the pressure range above 10^{-1} Torr.[15] The effect of the elevated gas temperature in helium afterglows is investigated in this paper. The time-varying gas temperature is determined from the frequency of standing acoustic waves excited by the gas dis-